

## Research Article

# Routh–Hurwitz Stability and Quasiperiodic Attractors in a Fractional-Order Model for Awareness Programs: Applications to COVID-19 Pandemic

Taher S. Hassan <sup>1,2,3</sup>, E. M. Elabbasy <sup>2</sup>, A.E. Matouk <sup>4,5</sup>, Rabie A. Ramadan <sup>6,7</sup>, Alanazi T. Abdulrahman <sup>1</sup> and Ismoil Odinaev <sup>8</sup>

<sup>1</sup>Department of Mathematics College of Science, University of Ha'il, Ha'il 2440, Saudi Arabia

<sup>2</sup>Department of Mathematics Faculty of Science, Mansoura University, Mansoura 35516, Egypt

<sup>3</sup>Section of Mathematics, International Telematic University Uninettuno, Corso Vittorio Emanuele II 39 00186 Roma, Italy

<sup>4</sup>Department of Mathematics College of Science Al-Zulfi, Majmaah University, Al-Majmaah 11952, Saudi Arabia

<sup>5</sup>College of Engineering, Majmaah University, Al-Majmaah 11952, Saudi Arabia

<sup>6</sup>College of Computer Science and Engineering, University of Ha'il, Ha'il 81481, Saudi Arabia

<sup>7</sup>Department of Computer Engineering Faculty of Engineering, Cairo University, Cairo 12613, Egypt

<sup>8</sup>Department of Automated Electrical Systems Ural Power Engineering Institute, Ural Federal University, Yekaterinburg 620002, Russia

Correspondence should be addressed to E. M. Elabbasy; [emelabbasy@mans.edu.eg](mailto:emelabbasy@mans.edu.eg)

Received 17 January 2022; Accepted 5 March 2022; Published 15 April 2022

Academic Editor: Binxiang Dai

Copyright © 2022 Taher S. Hassan et al. This is an open access article distributed under the Creative Commons Attribution License, which permits unrestricted use, distribution, and reproduction in any medium, provided the original work is properly cited.

This work explores Routh–Hurwitz stability and complex dynamics in models for awareness programs to mitigate the spread of epidemics. Here, the investigated models are the integer-order model for awareness programs and their corresponding fractional form. A non-negative solution is shown to exist inside the globally attracting set (GAS) of the fractional model. It is also shown that the disease-free steady state is locally asymptotically stable (LAS) given that  $R_0$  is less than one, where  $R_0$  is the basic reproduction number. However, as  $R_0 > 1$ , an endemic steady state is created whose stability analysis is studied according to the extended fractional Routh–Hurwitz scheme, as the order lies in the interval (0,2]. Furthermore, the proposed awareness program models are numerically simulated based on the predictor-corrector algorithm and some clinical data of the COVID-19 pandemic in KSA. Besides, the model's basic reproduction number in KSA is calculated using the selected data ( $R_0 = 1.977828168$ ). In conclusion, the findings indicate the effectiveness of fractional-order calculus to simulate, predict, and control the spread of epidemiological diseases.

## 1. Introduction

In late 2019, a severe respiratory syndrome, SARS-CoV-2, was detected in Wuhan, China, causing severe disease (COVID-19) [1]. Currently, COVID-19 has become a worldwide pandemic [2, 3]. Although some vaccines have already been announced, new mutant versions (such as COVID-19-VUI-2020/12/01) have recently been reported, which might have different features that reduce vaccines' effectiveness and help increase transmissibility and death rates.

Several epidemiological models (EMs) are reported to discuss the spread of COVID-19 and to better forecast the predictions in different countries. For example, Ben Fredj and Chrif presented a model to discuss the disease infection in Tunisia [4]. In [5], Ivorra et al. studied the spread of COVID-19 in China. COVID-19 statistical projections for China and Italy were provided by Alberti and Faranda [6] and, based on the SEIR model, Annas et al. investigated COVID-19 in Indonesia [7]. Furthermore, qualitative and quantitative dynamics have been studied in some recent

COVID-19 models. For example; Raza et al. proposed a model for coronavirus pandemic with a delay effect [8]. Abdul Razzaq et al. introduced an optimal control model to investigate the proficiency of each strategy in reducing the virulence of SARS-CoV-2 [9]. Chowdhury et al., proposed a mathematical model considering asymptomatic and symptomatic disease transmission processes in the COVID-19 outbreak so as to evaluate the effect of these transmissions on the virus [10]. Furthermore, Chowdhury et al. proposed another mathematical model to investigate the dynamics of viral load within the host by considering the role of T-cells and natural killer cells [11].

Fractional calculus has been shown to be an essential tool that has been used in different fields of science [12–27]. A fractional differential operator is called a nonlocal operator if it involves integration. The recently appearing and commonly used nonlocal fractional differential operators are the so-called Caputo's type [28] and Caputo–Fabrizio's type [29]. The nonlocal fractional operators are classified due to their kernels. Therefore, fractional modeling has great importance for epidemiological mathematical models because of its accuracy in describing natural phenomena and the existence of memory effects that are useful to describe the dynamical behaviors of biological phenomena. Consequently, the nonlocal fractional differential operators provide vital tools to describe the complexity existing in natural phenomena, especially in biological models and EMs. Recently, EMs with fractional derivatives have been reported. For example, Iqbal et al. studied a fractional-order model of HIV/AIDS infection [30]. Dokuyucu and Dutta investigated the Ebola virus based on Caputo–Fabrizio operator [31]. El-Sayed et al. studied a fractional-order model of plant diseases based on the Caputo operator [32]. Ameen et al. presented the problem of fractional optimal control for the SIRV epidemic model based on the left Caputo fractional derivative [33]. Naik et al. showed chaotic behaviors in an HIV-1 model with fractional order [34]. In addition, Kumar et al. reported chaotic dynamics in a fractional-order model of tumor-immune [35]. Meanwhile, some fractional-order models describing COVID-19 epidemiological models have recently appeared. For example, Singh et al. investigated the dynamics of a fractional-order model of COVID-19 [36]. Higazy introduced a new SIDARTHE model for COVID-19 with fractional derivatives [37]. Dong et al. [38] performed optimal control for a granular SEIR model using COVID-19 data. Tuan et al. [39] discussed the transmission of COVID-19 using a fractional mathematical model involving Caputo's type that contains a singular kernel. Zhang introduced new fractional-order models of COVID-19 involving singular and nonsingular kernels [40]. Yadav and Verma studied a fractional system of SARS-CoV-2 in the case of Wuhan [41].

Indeed, EMs are considered to be among the most important models in computational biology where susceptible and infected states are further investigated using analytical and/or numerical tools to study the spread of infectious diseases and provide awareness to people and health institutions. Additionally, the EMs are able to mimic the disease's impact on a variety of factors and levels, such as

humidity and temperature. Therefore, the models that describe the interaction between the susceptible, infected state variables and the variables of the awareness programs provide more effective awareness strategies to mitigate the spreading behaviors of infectious diseases or pandemics. This applies to SARS-CoV-2 and its variants, especially when vaccines are in early stages or will not soon be widely available. Recently, awareness models have been reported; For example, Sweilam et al. studied a mathematical model for awareness programs based on Atangana–Baleanu–Caputo (ABC) operators involving multiple time delays [42]. In [43], Misra et al. introduced a nonlinear dynamical system for the influence of awareness programs on the spread of infectious diseases such as flu. The aforementioned model is described by four coupled ordinary differential equations in which Misra et al. showed that awareness programs can be used to control the spread of an infectious disease, but the disease remains endemic according to immigration. Hence, this system is a candidate model to study the COVID-19 pandemic.

The advantages of the present study can be summarized as follows: complex dynamics, including quasiperiodic attractors, are explored in the integer-order awareness program model given by Misra et al. and its fractional-order version in the sense of the Caputo definition (as the fractional parameter lies above and below one). The suggested awareness models are shown to be applicable to some COVID-19 data collected from Saudi Arabia (KSA). So, the study of complex behaviors in such models enables governments to control and predict the development of epidemic diseases such as SARS-CoV-2, to give qualitative results, and to raise awareness of potentially critical situations in many nations with new variations.

Finally, to justify the main motivation of this work, we point out that the obtained results show that the fractional-order model is more suitable to handle such dynamics since the memory concept in the fractional counterpart erases oscillations in the curves of the model's steady states; it also flattens such curves so that the system as a whole settles on an equilibrium point faster than it would with the classic integer-order form.

## 2. Fractional Calculus

The nonlocal operator with a singular kernel given by Caputo [44] is described as

$$D^q \alpha(s) = \frac{\left( \int_0^s (s-\psi)^{n-q-1} \alpha^{(n)}(\psi) d\psi \right)}{\Gamma(n-q)}, \quad s \in \mathbb{R}^+, \quad (1)$$

where  $n-1 < q < n, q > 0$  and  $n \in \mathbb{N}$ . The notation  $\Gamma(\cdot)$  refers to the Euler's gamma and  $\alpha^{(n)}(\psi)$  denotes  $d^n \alpha(\psi)/d\psi^n$ . The Laplace transform of the Caputo derivative given in the last equation is described by

$$\ell\{D^q \alpha(t)\}(s) = \left\{ s^q \ell(\alpha)(s) - \sum_{k=0}^{n-1} s^{q-k-1} \alpha^{(k)}(0) \right\}. \quad (2)$$

*Definition 1.* The Mittag-Leffler function of the fractional parameter  $q$  appearing in the Caputo definition of fractional derivative is defined by  $E_q(t) = \sum_{m=0}^{\infty} t^m / \Gamma(1 + mq)$ .

Then, the following lemmas can be introduced:

**Lemma 1** (see [45]). *Let us assume that  $\eta(t) > 0$  is a continuous and differentiable real-valued function. Hence, for any  $t \geq t_0$ ,*

$$D^q \left[ \eta(t) - \eta^* - \eta^* \ln \frac{\eta(t)}{\eta^*} \right] \leq \left( 1 - \frac{\eta^*}{\eta(t)} \right) D^q \eta(t), \quad \eta^* \in R^+, \forall q \in (0, 1). \tag{3}$$

**Lemma 2** (see [46]). *For example, let us take the following autonomous system:*

$$D^q \eta(t) = f(\eta), \quad 0 < q < 1. \tag{4}$$

Also, let  $\Omega$  be a bounded closed set. Each solution that originates in the set  $\Omega$  remains in this set for every  $t$ . If  $\exists P(\eta): \Omega \rightarrow R$  with continuous first partial derivatives that fulfill the inequalities  $D^q P|_{(2)} \leq 0$ . In addition, let  $\Psi = \{D^q P|_{(2)} = 0, \eta \in \Omega\}$ , and let us assume that  $\Phi$  is the largest invariant set of  $\Psi$ . Then, every solution  $\eta(t)$  starts in  $\Omega$  approaches to  $\Phi$  as  $t$  tends to infinity. In particular, if  $\Phi = \{0\}$ , then  $\lim_{t \rightarrow \infty} \eta(t) = 0$ .

Henceforth, LAS denotes the locally asymptotically stable steady state  $\bar{X}$  for brevity. The point  $\bar{X}$  of the linearized  $n$ -dimensional fractional-order system is LAS, provided that

$$\frac{|\arg(\lambda_k)|}{2} > q\pi, \quad k = 1, \dots, n, \tag{5}$$

given that  $0 < q \leq 2$  [47] where  $\lambda_k$  is an eigenvalue of the system's Jacobian matrix.

### 3. The Awareness Program Models

The integer-order awareness program model [43] is given here as follows:

$$\begin{aligned} \frac{dx_1}{dt} &= a - dx_1 + Ex_2 + fx_3 - bx_1x_2 - cx_1x_4, \\ \frac{dx_2}{dt} &= -(E + h + d)x_2 + bx_1x_2, \\ \frac{dx_3}{dt} &= cx_1x_4 - (d + f)x_3, \\ \frac{dx_4}{dt} &= gx_2 - kx_4, \end{aligned} \tag{6}$$

where the state variables  $x_1, x_2, x_3, x_4$  refer to the susceptible population, infective population, and susceptible population with awareness and awareness programs' cumulative density, respectively. The explanation of these parameters are given as follows:

- (i)  $a$  is the recruitment rate
- (ii)  $b$  refers to infection contact rate
- (iii)  $c$  represents the dissemination rate of awareness
- (iv)  $d$  represents the natural death rate
- (v)  $E$  refers to the rate of recovery,
- (vi)  $f$  refers to a transfer rate of aware individuals to susceptible class,
- (vii)  $g$  represents awareness program implementation rate,
- (viii)  $h$  represents death rate according to infection,
- (ix)  $k$  denotes the program's depletion rate according to social problems and ineffectiveness.

All the parameter values are assumed to be positive. It is also believed that the density of the awareness program increases at a pace that is proportionate to the number of infected people in the population.

In fact, inserting the operator  $D^q$  into the awareness program model (6) allows us to better describe the natural phenomena, obtain more adequacy, and erase oscillations in the curves of the model's steady states. Therefore, the resulting fractional model is a better choice to handle complex dynamics. Consequently, the fractional counterpart of the awareness program model (6) is given by

$$\begin{aligned} D^q x_1 &= a - dx_1 + Ex_2 + fx_3 - bx_1x_2 - cx_1x_4, \\ D^q x_2 &= -(E + h + d)x_2 + bx_1x_2, \\ D^q x_3 &= cx_1x_4 - (d + f)x_3, \\ D^q x_4 &= gx_2 - kx_4, \end{aligned} \tag{7}$$

where  $q$  represents the fractional parameter satisfying  $q \in (0, 2]$ . The systems (6) and (7) have the following equilibria: the diseasefree point ( $S_0$ ) and the endemic point ( $S_1$ ). They are described as

$$S_0 = \left( \frac{a}{d}, 0, 0, 0 \right), \tag{8}$$

$$S_1 = (\beta_1, \beta_2, \beta_3, \beta_4),$$

where

$$\begin{aligned}\beta_1 &= \frac{d + E + h}{b}, \\ \beta_2 &= \frac{\rho k}{g}, \\ \beta_3 &= \frac{cg(h + E + d)(ab - d(E + h) - d^2)}{b\vartheta}, \\ \beta_4 &= \frac{g\rho}{g}, \\ \rho &= ab(d + f) - [dE f + d^2(E + h + f) + dfh + d^3], \\ \vartheta &= bdhk + bfhk + d^2(bk + cg) + bdfk \\ &\quad + cdEg + dgch > 0.\end{aligned}\tag{9}$$

We define  $R_0$  (basic reproduction number) for model (6) as follows (see ref. [43]):

$$R_0 = \frac{ab}{Ed + hd + d^2}.\tag{10}$$

Obviously, the endemic steady state  $S_1$  appears only if  $R_0 > 1$ .

*Remark 1.* It is easy to check that  $\rho > 0$  if  $R_0 > 1$ . Hence,  $\beta_4 > 0$ , when  $R_0 > 1$ .

*Remark 2.* We can easily check that  $\beta_2 > \beta_1$  if  $\rho kd/a\vartheta > Ed + hd + d^2/ab = 1/R_0$ . Hence,  $\beta_2 > \beta_1$  if

$$\frac{1}{R_0} < \frac{d}{a} \left\{ \frac{abk(d + f) - [dE f + d^2(E + h + f) + dfh + d^3]k}{bdhk + bfhk + d^2(bk + cg) + bdfk + cdEg + cfgh} \right\}.\tag{11}$$

To discuss the existence of non-negative solutions inside a globally attracting set (GAS) of the awareness program model (7) with  $q \in (0, 1)$ , one proves the following results:

**Theorem 1.** *Suppose that a closed set  $\Omega = \{(x_1, x_2, x_3, x_4) \in R_+^4: x_i \geq 0, i = 1, 2, 3, 4, S \leq a/\gamma\}$ , where  $x_i$  represents a state variable of the awareness programs model,  $S = \sum_{i=1}^4 x_i$  and  $\gamma = \min(d, k)$ , then  $\Omega$  is a positively invariant set and is GAS for the fractional-order awareness programs model (5) with  $0 < q < 1$ .*

*Proof.* It is evident that

$$D^q S(t) < a - \gamma S(t).\tag{12}$$

Applying the Laplace transform, the inequality (12) is reduced to

$$S(t) \leq \left( S(0) - \frac{a}{\gamma} \right) E_q(-\gamma t^q) + \frac{a}{\gamma},\tag{13}$$

where  $E_q(-\gamma t^q)$  represents the Mittag-Leffler function. So,  $E_q(-\gamma t^q) \leq 1$  is bounded. It is clear that  $S(t) \leq a/\gamma$  since  $S(0) \leq a/\gamma$ , hence the set  $\Omega$  of the awareness program model (7) is positive closed invariant. Now, since  $\lim_{t \rightarrow \infty} E_q(-\gamma t^q) = 0$ , then for a solution  $\Phi(t)$  of model (7) and  $S(0) > a/\gamma$ , one gets

$$\lim_{t \rightarrow \infty} \Phi(S(t)) = \frac{a}{\gamma}.\tag{14}$$

Thus,  $\Omega$  is GAS for the awareness program model (7) for all  $t > 0$ .  $\square$

#### 4. Local Stability

Here, conditions for the local stability of  $S_0$  and  $S_1$  are discussed. The Jacobian matrix of the awareness program models (6) and (7) are described as

$$J((x_1, x_2, x_3, x_4)) = \begin{pmatrix} -bx_2 - cx_4 - d & -bx_1 + E & f & -cx_1 \\ bx_2 & bx_1 - E - h - d & 0 & 0 \\ cx_4 & 0 & -d - f & cx_1 \\ 0 & g & 0 & -k \end{pmatrix}.\tag{15}$$

**Theorem 2.** *A diseasefree point  $S_0 = (a/d, 0, 0, 0)$  of the awareness program models (4) and (5) is LAS when  $R_0 < 1$ .*

*Proof.* The Jacobian matrix (11) computed at a diseasefree steady state  $S_0 = (a/d, 0, 0, 0)$  has the eigenvalues

$\lambda_1 = -d < 0, \lambda_2 = -k < 0, \lambda_3 = -d - f < 0, \lambda_4 = -Ed + h$   
 $d + d^2 - ab/d$ . Clearly,  $\lambda_1 < 0, \lambda_2 < 0, \lambda_3 < 0$  satisfy conditions  
 (5). Also,  $\lambda_4$  satisfies conditions (3), if  $R_0 < 1$ .  $\square$

To discuss the case of the endemic point  
 $S_1 = (\beta_1, \beta_2, \beta_3, \beta_4)$ , let us assume that its eigenvalue equa-  
 tion has the following form:

$$P(\lambda) = \lambda^4 + \mu_1\lambda^3 + \mu_2\lambda^2 + \mu_3\lambda + \mu_4 = 0, \tag{16}$$

where

$$\begin{aligned} \mu_1 &= h + E + 3d + k + f + b(\beta_2 - \beta_1) + c\beta_4, \\ \mu_2 &= (b(\beta_2 - \beta_1) + f + h + c\beta_4 + 3d + E)k + (b(\beta_2 - \beta_1) + E + h + 2d)f \\ &\quad + 2\left(\begin{matrix} 1.5d + E \\ +h + c\beta_4 + b(\beta_2 - \beta_1) \end{matrix}\right)d + bh\beta_2 + c(h + E - b\beta_1)\beta_4, \\ \mu_3 &= [(2d + E + h + b(\beta_2 - \beta_1))f + 3d^2 + 2(E + h + c\beta_4 + b(\beta_2 - \beta_1))d + bh\beta_2 + c(h + E - b\beta_1)\beta_4] \\ &\quad k + d^3 + (E + f + h + c\beta_4 + b(\beta_2 - \beta_1))d^2 + \left(\begin{matrix} bh\beta_2 + (E + h + b(\beta_2 - \beta_1))f \\ +c(E + h - b\beta_1)\beta_4 \end{matrix}\right)d + b\beta_2(fh + cg\beta_1), \\ \mu_4 &= \left[ (b d(\beta_2 - \beta_1) + (d + b\beta_2)h + f(d + E)d) + d^3 + (E + h + c\beta_4 + bd^2(\beta_2 - \beta_1)) \right] k + bcdg\beta_1\beta_2. \\ &\quad + d(bh\beta_2 + (h + E - b\beta_1)\beta_4c) \end{aligned} \tag{17}$$

Then, we assign the notation  $\Delta(P(\lambda))$  to refer to the  
 discriminant of the polynomial given in (16).

Obviously, the coefficients  $\mu_i > 0, i = 1, 2, 3, 4$ , if  $\beta_2 > \beta_1$ ,  
 $\beta_4 > 0$  and the quantity  $bh\beta_2 + c(h + E - b\beta_1)\beta_4 > 0$ . The last

inequality holds if  $b > c dg/hk$  and  $\rho > 0$ . So, according to  
 Remarks 1 and 2, the following lemma is easily proved:  $\square$

**Lemma 3.** *The coefficients  $\mu_i > 0, i = 1, 2, 3, 4$  when the  
 following inequalities hold*

$$\frac{1}{R_0} < \min \left\{ 1, \frac{d abk(d + f) - [dEf + d^2(E + h + f) + dfh + d^3]k}{a bdhk + b fhk + d^2(bk + cg) + bdfk + cdEg + c fgh} \right\}, b > \frac{cdg}{hk}. \tag{18}$$

The conditions of local stability of  $S_1$  is governed by the  
 fractional Routh-Hurwitz (FRH) criterion given by Matouk  
 [48, 49]:

(i) We define the Routh-Hurwitz determinants  
 $\Pi_1, \Pi_2, \Pi_3$  as follows:

$$\begin{aligned} \Pi_1 &= \mu_1, \\ \Pi_2 &= \begin{vmatrix} \mu_1 & 1 \\ \mu_3 & \mu_2 \end{vmatrix}, \\ \Pi_3 &= \begin{vmatrix} \mu_1 & 1 & 0 \\ \mu_3 & \mu_2 & \mu_1 \\ 0 & \mu_4 & \mu_3 \end{vmatrix}. \end{aligned} \tag{19}$$

If  $q \in (0, 2], \Pi_1 > 0, \Pi_2 > 0, \Pi_3 = 0$  and  $\mu_4 > 0$ , then  
 the endemic steady state  $S_1 = (\beta_1, \beta_2, \beta_3, \beta_4)$  is LAS.

(ii) If  $q \in (2/3, 2], \Delta(P(\lambda)) > 0, \mu_1 > 0$  and  $\mu_2 < 0$ , then  
 the endemic steady state  $S_1 = (\beta_1, \beta_2, \beta_3, \beta_4)$  does not  
 achieve the stability inequalities (3).

(iii) If  $q \in (0, 1/3), \Delta(P(\lambda)) < 0$  and the coefficients  
 $\mu_i > 0, i = 1, 2, 3, 4$  then the endemic steady state  
 $S_1 = (\beta_1, \beta_2, \beta_3, \beta_4)$  is LAS. Also, if  
 $q \in (0, 2], \Delta(P(\lambda)) < 0, \mu_1 < 0, \mu_3 < 0, \mu_2 > 0$  and  
 $\mu_4 > 0$ , then the endemic steady state  
 $S_1 = (\beta_1, \beta_2, \beta_3, \beta_4)$  does not achieve the stability  
 inequalities (3).

(iv) If  $q \in (0, 1), \Delta(P(\lambda)) < 0$ , the coefficients  $\mu_i > 0, i =$   
 $1, 2, 3, 4$  and  $\mu_3/\mu_1\mu_2 + \mu_1\mu_4/\mu_2\mu_3 = 1$  then the en-  
 demic steady state  $S_1 = (\beta_1, \beta_2, \beta_3, \beta_4)$  is LAS.  
 However, if  $q \in [1, 2], \Delta(P(\lambda)) < 0$  and  
 $\mu_3/\mu_1\mu_2 + \mu_1\mu_4/\mu_2\mu_3 = 1$ , then the conditions (3)  
 are not satisfied by the endemic steady state.

(v) If  $q \in (0, 2],$  then  $\mu_4 > 0$  is an imperative condition  
 for the endemic steady state  $S_1 = (\beta_1, \beta_2, \beta_3, \beta_4)$  to be  
 LAS.

Accordingly, the following lemma is easily proved:

**Lemma 4.** *If the following inequalities hold*

$$\frac{1}{R_0} < \min \left\{ 1, \frac{d \text{ abk}(d+f) - [dEf + d^2(E+h+f) + dfh + d^3]k}{a \text{ bdhk} + b \text{ fhk} + d^2(bk+cg) + bdfk + cdEg + cfgh} \right\}, b > \frac{cdg}{hk}, \quad (20)$$

the endemic steady state  $S_1 = (\beta_1, \beta_2, \beta_3, \beta_4)$  of the fractional awareness programs model (7) exists and is LAS given that

- (i)  $0 < q \leq 2, \Pi_i > 0, i = 1, 2$  and  $\Pi_3 = 0$ ,
- (ii)  $q \in (0, 1/3)$  and  $\Delta(P(\lambda)) < 0$ ,
- (iii)  $q \in (0, 1), \Delta(P(\lambda)) < 0$ , and  
 $\mu_3/\mu_1\mu_2 + \mu_1\mu_4/\mu_2\mu_3 = 1$ .

*Remark 3* (see [43]). For  $q = 1, R_0 > 1$ , then the endemic steady state  $S_1 = (\beta_1, \beta_2, \beta_3, \beta_4)$  is LAS if

$$\frac{3c^2}{(c\beta_4 + d + f)^2} < \min \left\{ \frac{1}{3\beta_4^2}, \frac{d}{\alpha\beta_4^2}, \frac{2k^2}{9g^2(\beta_3 - \beta_1 - \beta_2)^2} \right\}. \quad (21)$$

## 5. Numerical Simulations in the Awareness Program Model

Numerical simulations are performed for the awareness program model (6) to produce four attractors with different topologies. The initial conditions are selected as  $x_1(t) = 1, x_2(t) = 0.1, x_3(t) = 0.003$ , and  $x_4(t) = 0.002$ . The numerical simulations are based on four sets of parameter values. We define a parameter set as  $\{a, b, c, d, E, f, g, h, k\}$ , then

$$\begin{aligned} A &= \{0.16, 0.99, 0.75, 0.02, 0.96, 0.08, 0.95, 0.45, 0.2\}, \\ B &= \{0.22, 0.95, 0.90, 0.02, 0.96, 0.05, 0.95, 0.95, 0.3\}, \\ C &= \{0.45, 0.95, 0.90, 0.01, 0.96, 0.05, 0.95, 0.95, 0.3\}, \\ D &= \{0.60, 0.95, 0.90, 0.01, 0.96, 0.05, 0.95, 0.95, 0.3\}. \end{aligned} \quad (22)$$

The computations of the eigenvalues corresponding to the parameter mentioned in above sets are given by the following tables:

With the aid of Table 1, it is clear that the eigenvalue  $\lambda_4 > 0$  for all the abovementioned sets of parameters. So, the diseasefree point of system (6) is not stable using these selections of parameter values. Moreover, Table 2 shows that the endemic point is unstable when the parameters are selected according to sets A and B. Furthermore, the endemic point is LAS when the parameters are selected according to sets C and D.

In fact, quasiperiodic behaviors occur in 4D systems when at least two maximal Lyapunov exponents (LEs) are vanishing or very close to zero. It is observed that quasiperiodic attractors are obtained using the selections of parameter sets A and B. The corresponding LEs are computed in Table 3 based on Wolf's algorithm [50]. The attractors

corresponding to the abovementioned parameter sets are also depicted in Figure 1, in which Figures 1(a) and 1(b) illustrate quasiperiodic attractors. To further discuss the existence of complex dynamics in system (6), we also show that the coexistence of multiattractors occurs using the selections of parameter sets A and B as depicted in Figure 2. The aforementioned figure shows unstable focus-node attractor (blue domain) coexists with a quasiperiodic attractor (red domain).

The spectrum of LEs related to parameter sets A and B with varying parameter  $a$  is illustrated in Figure 3. Calculations of the bifurcation diagrams are also illustrated in Figure 4 where weak chaotic behaviors are shown in Figure 4(c).

## 6. Numerical Simulations in the Awareness Programs Model (7)

The fractional-order model (7) is also numerically integrated using the predictor-corrector algorithm [51, 52] with the parameter sets and initial conditions mentioned above. According to Table 1 and conditions (5), the diseasefree point of the fractional-order model (7) is not LAS. In addition, according to Table 2 and conditions (5), the endemic point is LAS when the parameters are selected according to the sets C and D. However, based on Table 2, the endemic point is not LAS if

$$q > \frac{2}{\pi} \arctan \left( \frac{\text{Im}(\lambda_{3,4})}{\text{Re}(\lambda_{3,4})} \right). \quad (23)$$

Quasiperiodic attractors are found using the parameter set A with fractional parameter  $q = 0.999$  and the parameter set B with fractional parameter  $q = 0.97$ . The obtained attractors corresponding to the numerical integration of the awareness programs model (7) with the sets A, B, C, and D are illustrated in Figure 5 in which quasiperiodic attractors are given by Figures 5(a) and 5(b). Moreover, computations of the LEs' spectrum of the fractional-order model (7) is carried out using the efficient algorithm by Danca and Kuznetsov [53]. The results are shown in Figures 6 and 7. Computations of the corresponding bifurcation diagrams are given in Figure 8. Furthermore, computations of the LEs of the fractional model, based on the algorithm by Danca and Kuznetsov, is described by Table 4.

Complex dynamics in the awareness programs model (7) are also obtained when  $q$  becomes greater than one. In Figures 9–11, the complex dynamics in the fractional awareness system (7) are depicted with the orders 1.07, 1.15, and using different sets of initial states.

TABLE 1: Computations of the eigenvalues ( $\lambda_{i,s}$ ) corresponding to the diseasefree point of the integer-order awareness program model (4).

Parameter set	$\lambda_1$	$\lambda_2$	$\lambda_3$	$\lambda_4$
A	-0.02	-0.1	-0.2	6.49
B	-0.02	-0.07	-0.3	8.52
C	-0.01	-0.06	-0.3	40.83
D	-0.01	-0.06	-0.3	55.08

TABLE 2: Computations of the eigenvalues ( $\lambda_{i,s}$ ) corresponding to the endemic point of the integer-order awareness program model (4). It is assumed that  $I = \sqrt{-1}$ .

Parameter set	$\lambda_1$	$\lambda_2$	$\lambda_3$	$\lambda_4$
A	-0.6952	-0.0257	$0.0014 + 0.3812I$	$0.0014 - 0.3812I$
B	-0.6784	-0.0266	$0.0276 + 0.4448I$	$0.0276 - 0.4448I$
C	-1.1242	-0.0167	$-0.0398 + 0.6235I$	$-0.0398 - 0.6235I$
D	-1.3501	-0.0167	$-0.0753 + 0.6579I$	$-0.0753 - 0.6579I$

TABLE 3: Computations of LEs ( $\Lambda_{i,s}$ ) of the integer-order awareness program model (6).

Parameter set	$\Lambda_1$	$\Lambda_2$	$\Lambda_3$	$\Lambda_4$
A	0.023980	-0.017883	-0.037342	-0.605040
B	0.012408	0.005288	-0.072330	-0.599232

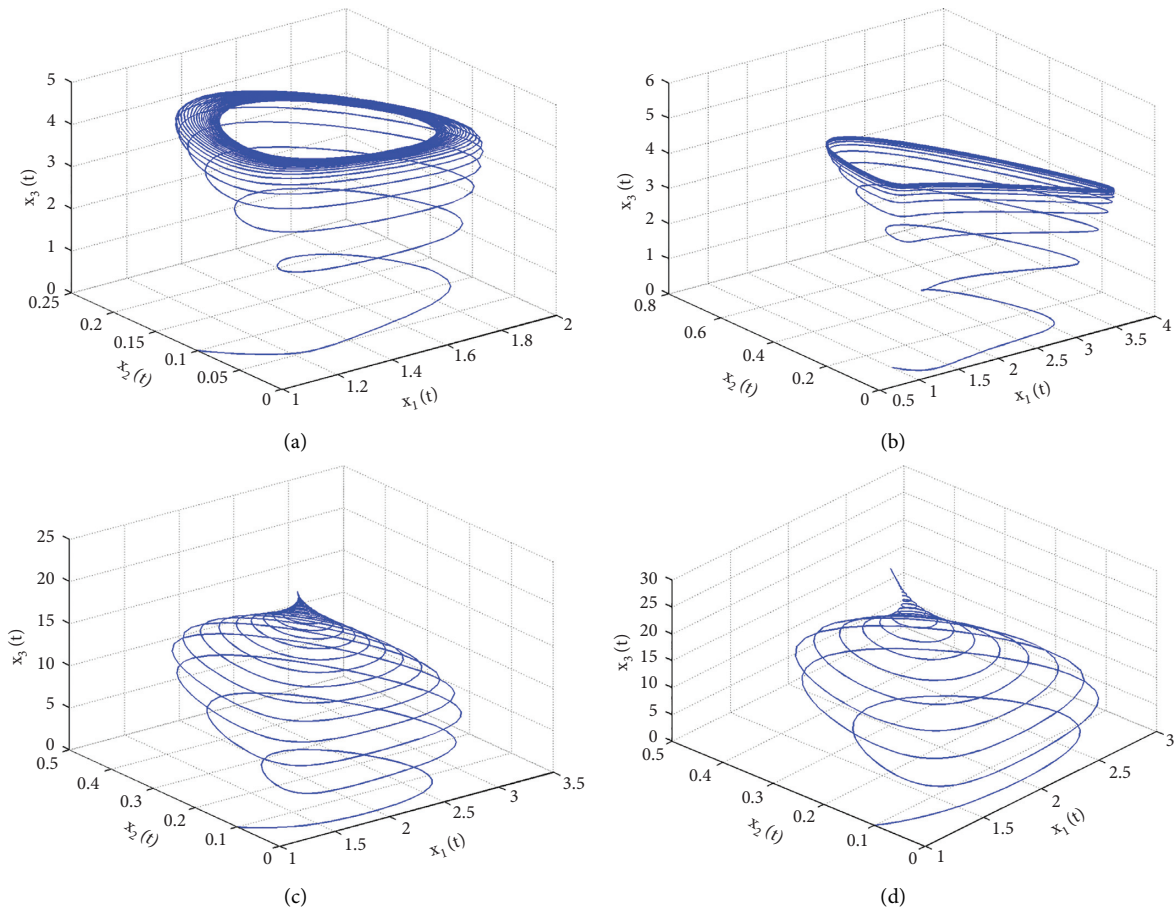


FIGURE 1: Three-dimensional plots of the awareness program model (6) using the parameter set: (a) A; (b) B; (c) C; and (d) D.

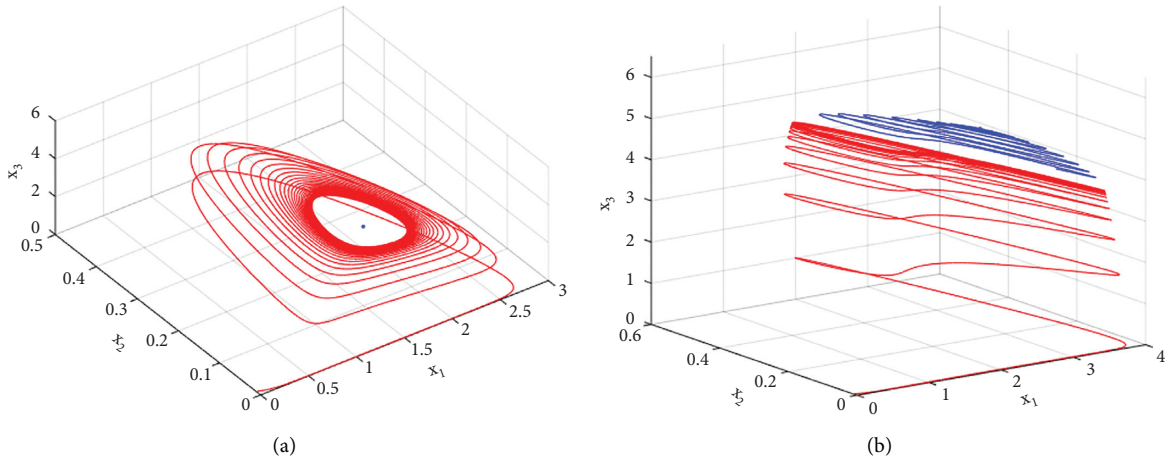


FIGURE 2: Coexistence of multiattractors in the awareness program system (6) using the parameter sets: (a)  $A$  with initial conditions  $(0.01, 0.01, 0.01, 0.01)^T$  for red trajectory;  $(1.4444, 0.087455, 4.50033, 0.415416)^T$  for blue trajectory; and (b)  $B$  with initial conditions  $(0.01, 0.01, 0.01, 0.01)^T$  for red trajectory;  $(2.03157, 0.068349, 5.65347, 0.216439)^T$  for blue trajectory.

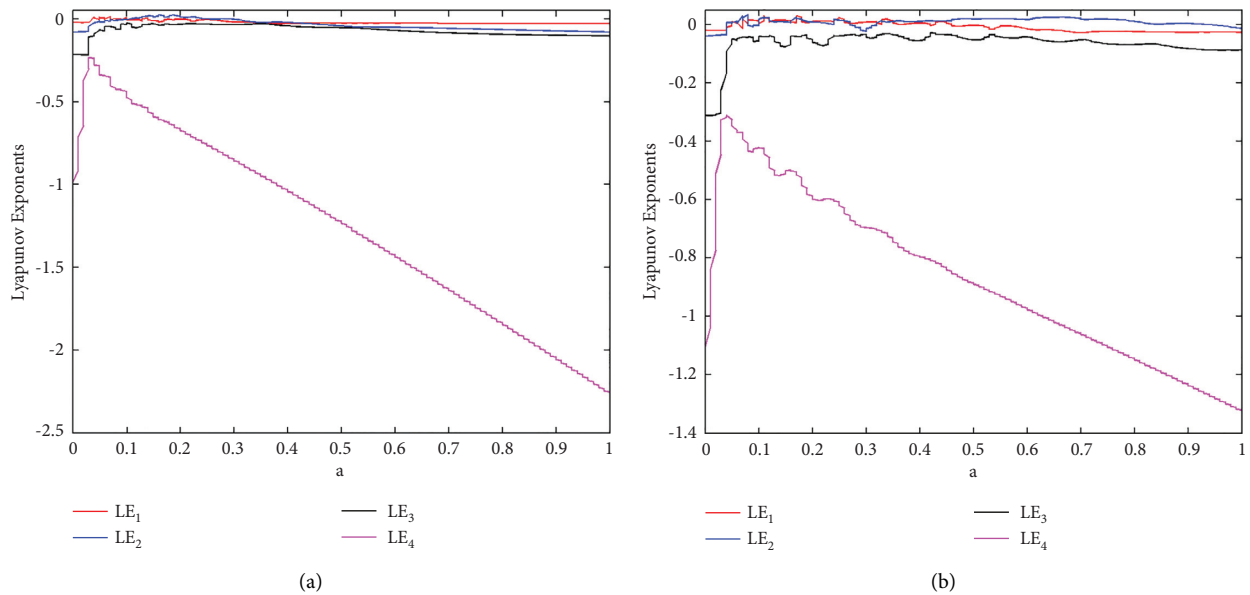


FIGURE 3: Lyapunov spectrum of the awareness program model (6) vs.  $a$  and fixing other values in the parameter set: (a)  $A$  and (b)  $B$ .

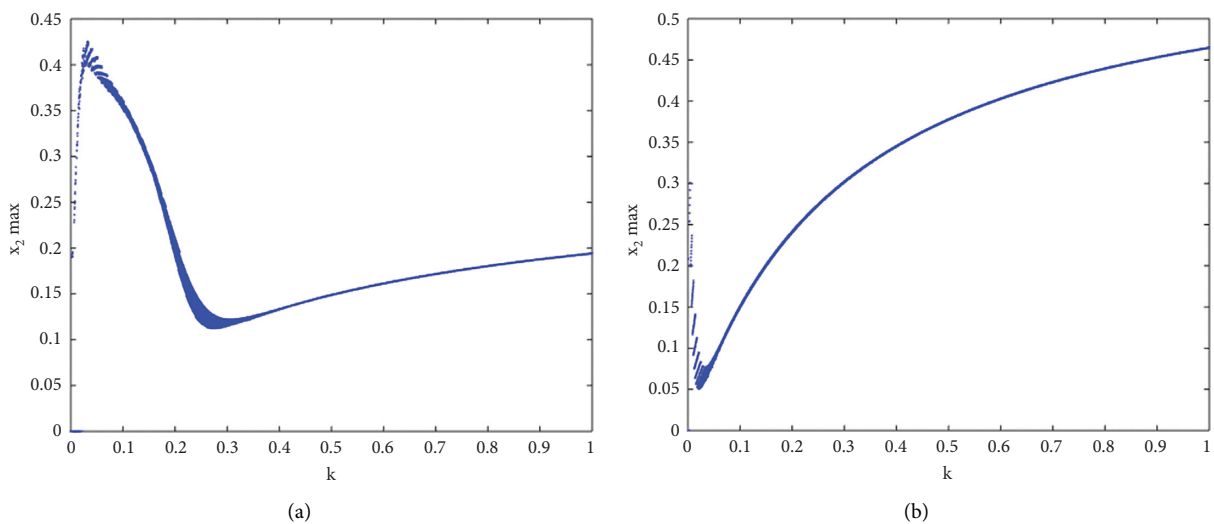


FIGURE 4: Continued.



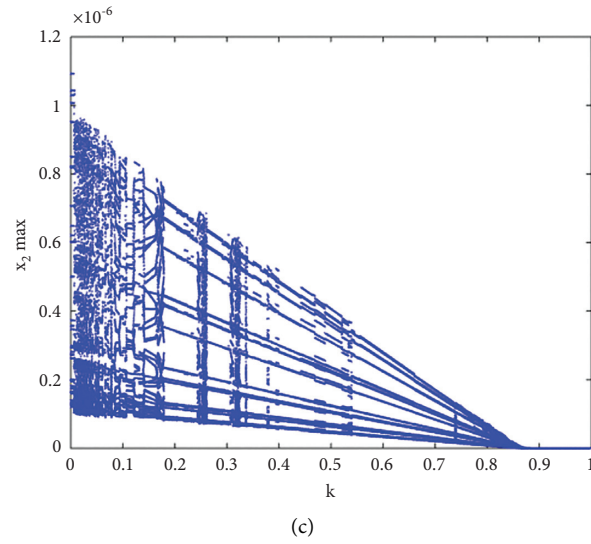


FIGURE 4: Bifurcation diagrams of the awareness program model (6) vs.  $k$  and fixing other values in the parameter set: (a) A; (b) B; and (c) D.

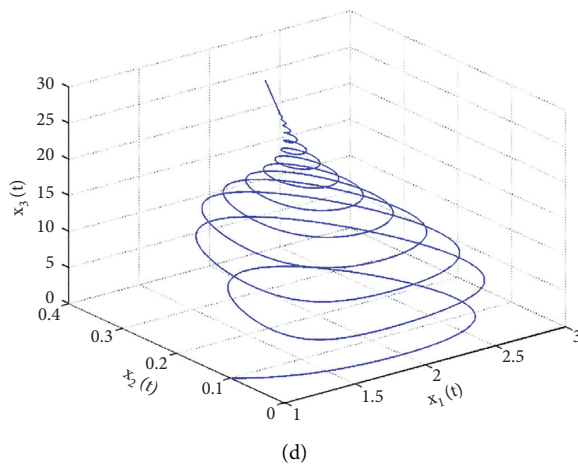
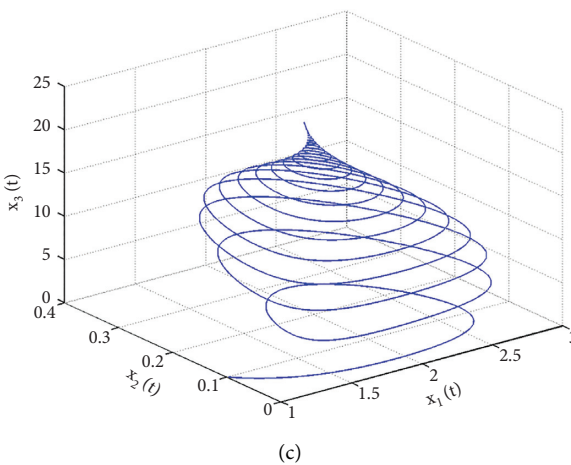
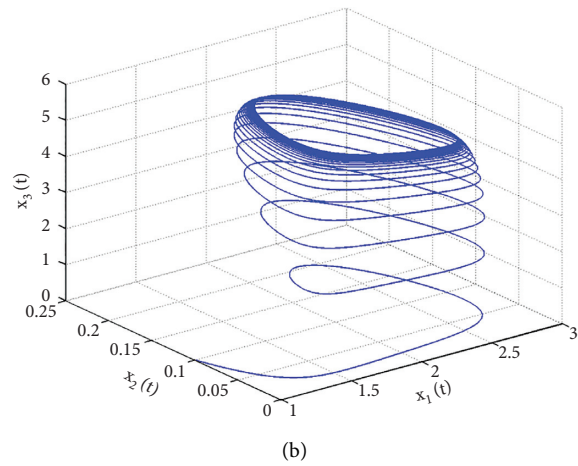
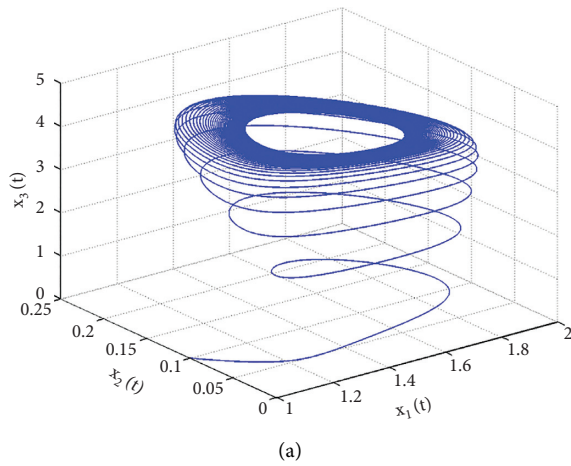


FIGURE 5: Three-dimensional plots of the awareness program model (7) using the parameter sets: (a) A and the fractional-order 0.999; (b) B and the fractional-order 0.97; (c) C and the fractional-order 0.99; and (d) D and the fractional-order 0.99.

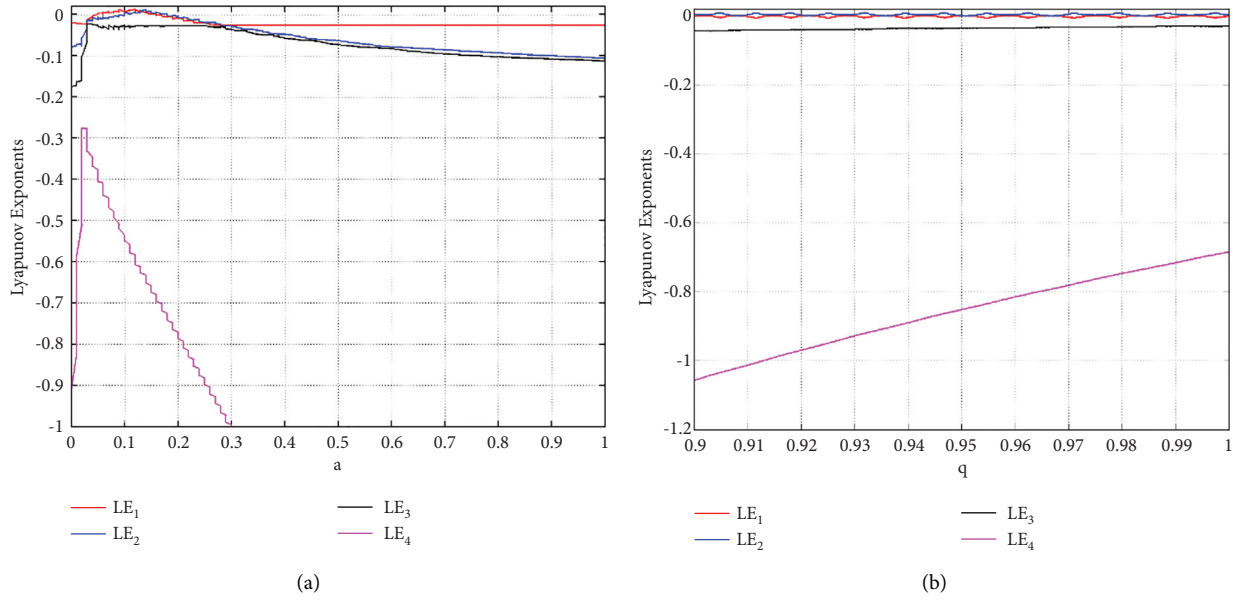


FIGURE 6: Lyapunov spectrum of awareness program model (7) with (a)  $q = 0.999$ , the parameter set A and varying  $a$  and (b) the parameter set A and varying  $q$ .

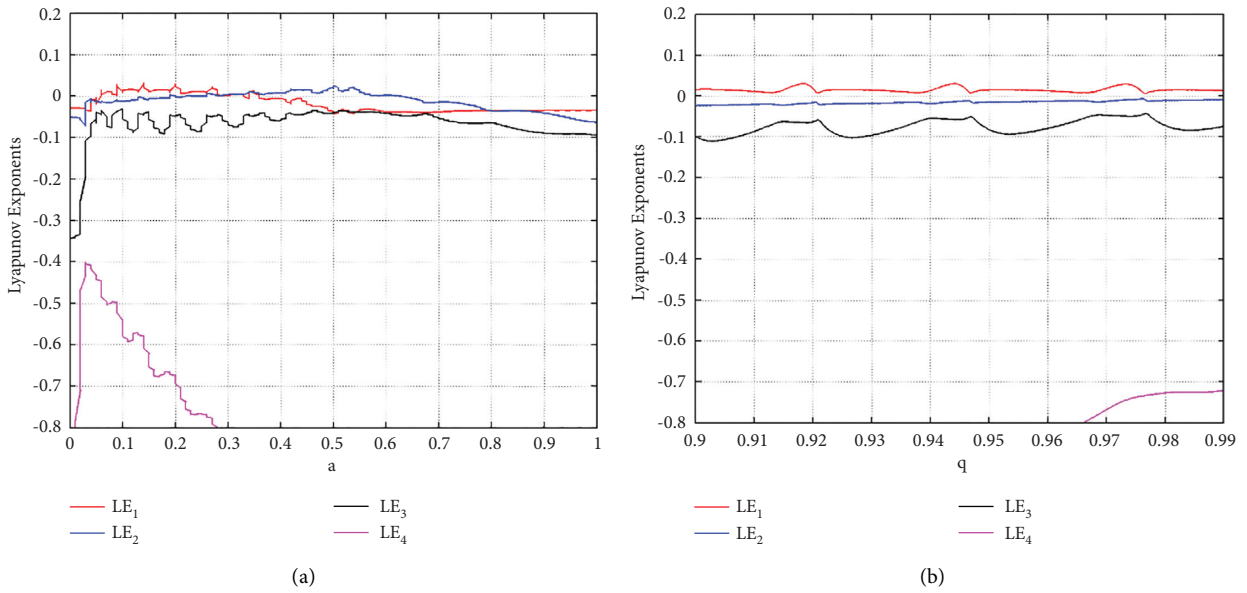


FIGURE 7: Lyapunov spectrum of awareness program model (7) with (a)  $q = 0.97$ , the parameter set B and varying  $a$  and (b) the parameter set B and varying  $q$ .

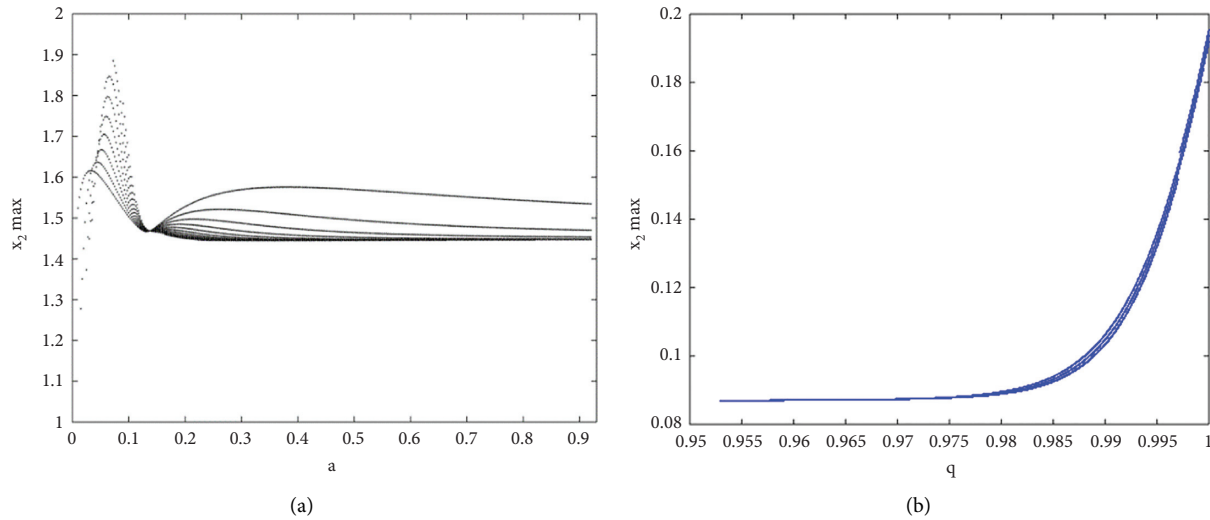


FIGURE 8: Bifurcation diagram of the awareness programs model (7) (a) vs. the dynamical parameter  $a$  and fixing other values in the parameter set  $A$  and (b) vs. the fractional-order  $q$  and using the parameter set  $A$ .

TABLE 4: Computations of LEs ( $\Lambda_{i,s}$ ) of the fractional-order awareness programs model (7) with initial conditions  $x_1(0) = 1.2, x_2(0) = 0.11, x_3(0) = 4, x_4(0) = 0.2646$  and  $x_1(0) = 2, x_2(0) = 0.18, x_3(0) = 5.6, x_4(0) = 0.16$ , respectively.

Parameter set and fractional order	$\Lambda_1$	$\Lambda_2$	$\Lambda_3$	$\Lambda_4$
Set $A$ and $q = 0.999$	0.0043	-0.0001	-0.0280	-0.6853
Set $B$ and $q = 0.97$	0.0089	-0.0005	-0.0684	-0.7560

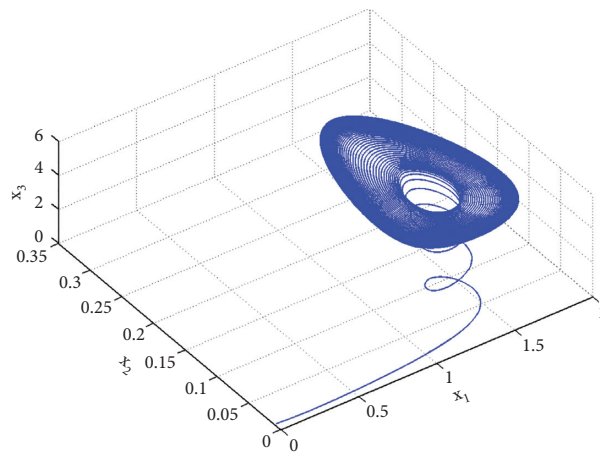


FIGURE 9: Three-dimensional plots of the fractional model (7) using the parameter set  $A$ , the fractional-order  $q = 1.07$ , and using initial conditions  $(0.01, 0.01, 0.01, 0.01)^T$ .

### 7. Discussion and Conclusion

This section examines some COVID-19 data obtained for KSA [54–56] and collected over the period from March 18 to August 15, 2020. The initial value of the total population is  $N(0) = 37 \times 10^6$ , which is divided into three classes  $x_1(0), x_2(0), x_3(0)$ . Also, confirmed cases are  $299 \times 10^3$ , recovered cases are  $267 \times 10^3$ , and the number of deaths due to infection is 3408. In addition, the natural death rate in KSA is approximately 3.5 per 1000 people. Based on the model’s assumptions and the collected data of COVID-19, the following selection of parameter values is tested via numerical

simulations  $E = \{400, 0.0000157, 0.0002, 0.0035, 0.8923, 0.2, 0.0005, 0.0114, 0.06\}$ . Basic reproduction ratio  $R_0$  is also computed as follows:

$$R_0 = 1.977828168 > 1. \tag{24}$$

So, the point  $S_0$  is not LAS. However, the endemic steady state  $S_1 = (57783.43949, 11944.52854, 5652.710421, 99.53773787)$  is LAS since all the eigenvalues satisfy the conditions (5). Moreover, the discriminant of the eigenvalue equation of the endemic point is calculated as  $\Delta(P(\lambda)) = -0.2883978794 \times 10^{-9} < 0$ , which implies that the

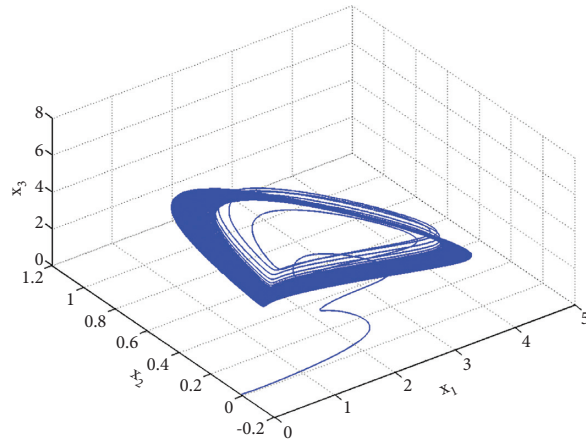


FIGURE 10: Three-dimensional plots of the fractional model (7) using the parameter set  $B$ , the fractional-order  $q = 1.15$ , and using initial conditions  $(0.01, 0.01, 0.01, 0.01)^T$ .

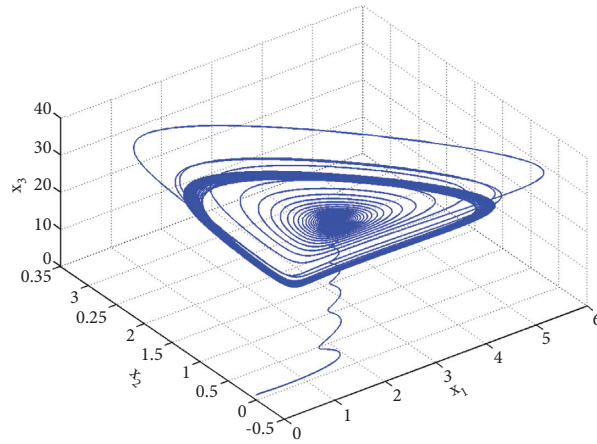


FIGURE 11: Three-dimensional plots of the fractional model (7) using the parameter set  $D$ , the fractional-order  $q = 1.15$ , and using initial conditions  $(0.085, 0.085, 0.085, 0.085)^T$ .

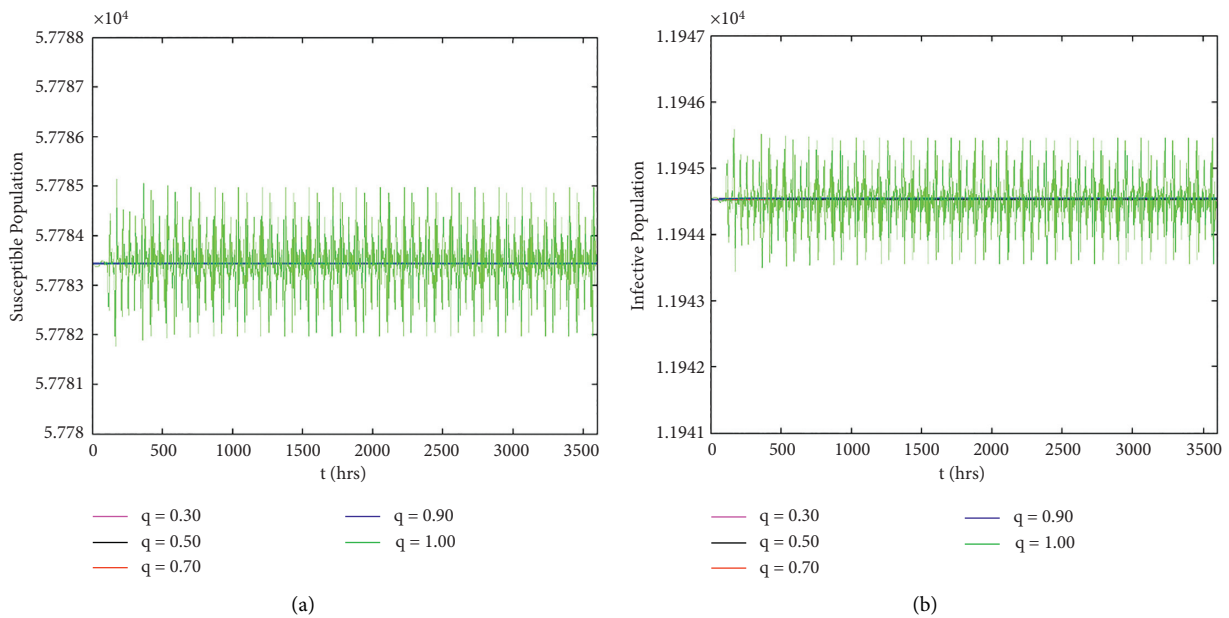


FIGURE 12: Continued.

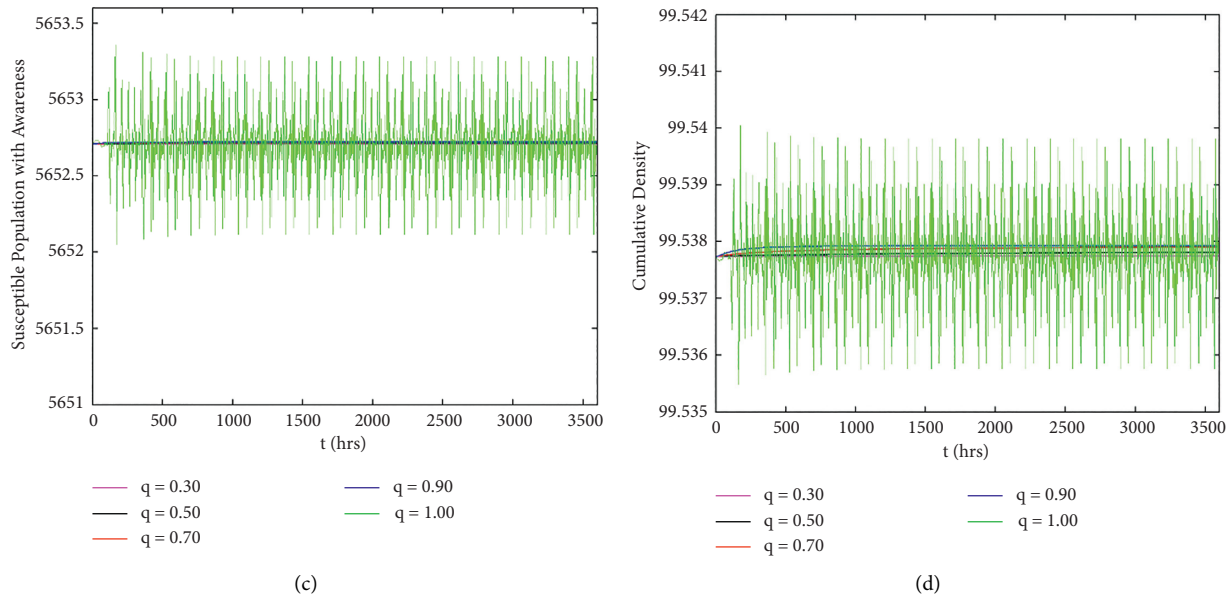


FIGURE 12: Variation of the state variables of the awareness program models (6) and (7) with time using different values of the fractional parameter and using the set E.

endemic state has two complex conjugate eigenvalues. Obviously, the first statement of the FRH stability condition (iii) is also satisfied when  $q < 1/3$ . The simulation results illustrate that the model (5) approaches the endemic steady state quicker than its integer-order form (see Figure 12). Here, the memory effect in the fractional-order model erases the oscillations in its integer-order counterpart after a few times, which makes the fractional awareness program model as a whole settle on the endemic point quicker than it would with the integer-order version. Therefore, the fractional system (5) is more suitable for investigating the awareness program model dynamics using the abovementioned data of COVID-19.

On the other hand, the higher degrees of freedom existing in the fractional model of awareness programs can be treated as controllers to stabilize its state variables to the targeted endemic steady state. Besides, the fractional parameters are flattening the curves in Figure 12, which can be used as a good public health strategy to mitigate or slow down the spread of COVID-19. Hence, the fractional models achieve more adequacy in estimating the control measures that affect the spread of SARS-CoV-2 in KSA. Indeed, KSA presented awareness programs like issuing guidelines in different languages to raise people's awareness about necessary precautions against COVID-19 [57]. The guidelines include basic information about COVID-19 like symptoms, methods of transmission, and how to prevent it through providing full details on methods of using protective equipment on individuals (such as the proper way to wear the mask, gloves, overall gown, and wash hands), tips for traveling, the procedure of self-isolation in-home and quarantine, and medical treatment upon the appearance of respiratory symptoms. These programs were prepared by MOH in KSA and were broadcasted in different ways, like TV, newspapers, official websites, and street banners. The

reported guidelines show positive results in controlling the spread of SARS-CoV-2 in KSA.

In conclusion, the existence of a nonlocal fractional operator makes a fractional version of the awareness program model a better choice to predict, control, and handle its rich variety of complex dynamics and obtain better adequacy than the integer version. The resulting higher degrees of freedom in the fractional version also play an important role in displaying a rich variety of complex dynamics.

## Data Availability

The numerical data used to support the findings of this study are included in the article.

## Conflicts of Interests

The authors declare that there are no conflicts of interest with this study. There are no non-financial competing interests (political, personal, religious, ideological, academic, intellectual, commercial, or any other) to declare in relation to this manuscript.

## Authors' Contributions

Matouk directed the study and helped with the inspection. All the authors carried out the main results of this article, drafted the manuscript, and read and approved the final manuscript.

## Acknowledgments

This research has been funded by the Scientific Research Deanship at University of Ha'il - Saudi Arabia through project number RG-21 011.

## References

- [1] P. Zhou, X. L. Yang, X. G. Wang, B. Hu, L. Zhang, and W. Zhang, "A pneumonia outbreak associated with a new coronavirus of probable bat origin," *Nature*, vol. 579, 2020.
- [2] F. Wu, "A new coronavirus associated with human respiratory disease in China," *Nature*, vol. 579, pp. 1–10, 2020.
- [3] Q. Lin, S. Zhao, D. Gao et al., "A conceptual model for the coronavirus disease 2019 (COVID-19) outbreak in Wuhan, China with individual reaction and governmental action," *International Journal of Infectious Diseases*, vol. 93, pp. 211–216, 2020.
- [4] H. Ben Fredj and F. Chrif, "Novel Corona virus disease infection in Tunisia: mathematical model and the impact of the quarantine strategy," *Chaos, Solitons & Fractals*, vol. 138, 2020.
- [5] B. Ivorra, M. R. Ferrández, M. Vela-Pérez, and A. M. Ramos, "Mathematical modeling of the spread of the coronavirus disease 2019 (COVID-19) taking into account the undetected infections. The case of China," *Communications in Nonlinear Science and Numerical Simulation*, vol. 88, p. 105303, 2020.
- [6] T. Alberti and D. Faranda, "On the uncertainty of real-time predictions of epidemic growths: a COVID-19 case study for China and Italy," *Communications in Nonlinear Science and Numerical Simulation*, vol. 90, p. 105372, 2020.
- [7] S. Annas, M. Isbar Pratama, M. Rifandi, W. Sanusi, and S. Side, "Stability analysis and numerical simulation of SEIR model for pandemic COVID-19 spread in Indonesia," *Chaos, Solitons, and Fractals*, vol. 139, Article ID 110072, 2020.
- [8] A. Raza, A. Ahmadian, M. Rafiq, S. Salahshour, and M. Ferrara, "An analysis of a nonlinear susceptible-exposed-infected-quarantine-recovered pandemic model of a novel coronavirus with delay effect," *Results in Physics*, vol. 21, Article ID 103771, 2021.
- [9] O. Abdul Razzaq, D. Ur Rehman, N. A. Khan, A. Ahmadian, and M. Ferrara, "Optimal surveillance mitigation of COVID-19 disease outbreak: fractional order optimal control of compartment model," *Results in Physics*, vol. 20, Article ID 103715, 2021.
- [10] S. M. E. K. Chowdhury, M. Forkan, S. F. Ahmed, P. Agarwal, A. B. M. Shawkat Ali, and S. M. Mueen, "Modeling the SARS-CoV-2 parallel transmission dynamics: asymptomatic and symptomatic pathways," *Computers in Biology and Medicine*, vol. 143, Article ID 105264, 2022.
- [11] S. M. E. K. Chowdhury, J. T. Chowdhury, J. T. Chowdhury, S. F. Ahmed, P. Badruddin, and S. Kamangar, "Mathematical modelling of COVID-19 disease dynamics: interaction between immune system and SARS-CoV-2 within host," *AIMS Mathematics*, vol. 7, no. 2, pp. 2618–2633, 2022.
- [12] A. E. Matouk, "A novel fractional-order system: chaos, hyperchaos and applications to linear control," *JAppl Comp Mech*, vol. 7, no. 2, pp. 701–714, 2021.
- [13] E. Ahmed and A. E. Matouk, "Complex dynamics of some models of antimicrobial resistance on complex networks," *Mathematical Methods in the Applied Sciences*, vol. 44, no. 2, pp. 1896–1912, 2021.
- [14] A. E. Matouk, "Chaos, feedback control and synchronization of a fractional-order modified Autonomous Van der Pol-Duffing circuit," *Communications in Nonlinear Science and Numerical Simulation*, vol. 16, no. 2, pp. 975–986, 2011.
- [15] A. S. Hegazi and A. E. Matouk, "Dynamical behaviors and synchronization in the fractional order hyperchaotic Chen system," *Applied Mathematics Letters*, vol. 24, no. 11, pp. 1938–1944, 2011.
- [16] V. Kiryakova and F. Mainardi, "Recent history of fractional calculus," *Communications in Nonlinear Science and Numerical Simulation*, vol. 16, pp. 1140–1153, 2011.
- [17] E. Ahmed and A. S. Elgazzar, "On fractional order differential equations model for nonlocal epidemics," *Physica A: Statistical Mechanics and Its Applications*, vol. 379, no. 2, pp. 607–614, 2007.
- [18] A. S. Hegazi, E. Ahmed, and A. E. Matouk, "On chaos control and synchronization of the commensurate fractional order Liu system," *Communications in Nonlinear Science and Numerical Simulation*, vol. 18, no. 5, pp. 1193–1202, 2013.
- [19] J. A. Tenreiro Machado and M. E. Mata, "Pseudo Phase Plane and Fractional Calculus modeling of western global economic downturn," *Communications in Nonlinear Science and Numerical Simulation*, vol. 22, pp. 396–406, 2015.
- [20] A. E. Matouk, A. A. Elsadany, E. Ahmed, and H. N. Agiza, "Dynamical behavior of fractional-order Hastings-Powell food chain model and its discretization," *Communications in Nonlinear Science and Numerical Simulation*, vol. 27, pp. 153–167, 2015.
- [21] A. E. Matouk, "Chaos synchronization of a fractional-order modified Van der Pol-Duffing system via new linear control, backstepping control and Takagi-Sugeno fuzzy approaches," *Complexity*, vol. 21, pp. 116–124, 2016.
- [22] A. E. Matouk and A. A. Elsadany, "Dynamical analysis, stabilization and discretization of a chaotic fractional-order GLV model," *Nonlinear Dynamics*, vol. 85, no. 3, pp. 1597–1612, 2016.
- [23] M. A. E. Herzallah and D. Baleanu, "Fractional-order Euler-Lagrange equations and formulation of Hamiltonian equations," *Nonlinear Dynamics*, vol. 58, no. 2, pp. 385–391, 2009.
- [24] A. E. Matouk, *Advanced Applications of Fractional Differential Operators to Science and Technology*, IGI Global, Pennsylvania, United States, 2020.
- [25] A. Al-khedhairi, A. E. Matouk, and I. Khan, "Chaotic dynamics and chaos control for the fractional-order geomagnetic field model," *Chaos, Solitons & Fractals*, vol. 128, pp. 390–401, 2019.
- [26] A. Al-khedhairi, A. E. Matouk, and S. S. Askar, "Computations of synchronization conditions in some fractional-order chaotic and hyperchaotic systems," *Pramana - Journal of Physics*, vol. 92, no. 72, p. 11, 2019.
- [27] S. Kumar, A. E. Matouk, H. Chaudhary, and S. Kant, "Control and synchronization of fractional-order chaotic satellite systems using feedback and adaptive control techniques," *International Journal of Adaptive Control and Signal Processing*, vol. 35, no. 4, pp. 484–497, 2021.
- [28] M. Caputo, "Linear models of dissipation whose Q is almost frequency independent--II," *Geophysical Journal International*, vol. 13, no. 5, pp. 529–539, 1967.
- [29] M. Caputo and M. Fabrizio, "A new definition of fractional derivative without singular kernel," *Prog Fract Differ Appl*, vol. 1, pp. 73–85, 2015.
- [30] Z. Iqbal, N. Ahmed, D. Baleanu, W. Adel, M. Rafiq, and M. A. Rehman, "Positivity and boundedness preserving numerical algorithm for the solution of fractional nonlinear epidemic model of HIV/AIDS transmission," *Chaos, Solitons & Fractals*, vol. 134, Article ID 109706, 2020.
- [31] M. A. Dokuyucu and H. Dutta, "A fractional order model for Ebola Virus with the new Caputo fractional derivative without singular kernel," *Chaos, Solitons & Fractals*, vol. 134, Article ID 109717, 2020.
- [32] A. M. A. El-Sayed, S. Z. Rida, and Y. A. Gaber, "Dynamical of curative and preventive treatments in a two-stage plant

- disease model of fractional order,” *Chaos, Solitons & Fractals*, vol. 137, Article ID 109879, 2020.
- [33] I. Ameen, D. Baleanu, and H. M. Ali, “An efficient algorithm for solving the fractional optimal control of SIRV epidemic model with a combination of vaccination and treatment,” *Chaos, Solitons & Fractals*, vol. 137, Article ID 109892, 2020.
- [34] P. A. Naik, K. M. Owolabi, M. Mehmet Yavuz, and J. Zu, “Chaotic dynamics of a fractional order HIV-1 model involving AIDS-related cancer cells,” *Chaos, Solitons & Fractals*, vol. 140, Article ID 110272, 2020.
- [35] S. Kumar, A. Kumar, B. Samet, J. F. Gómez-Aguilar, and M. S. Osman, “A chaos study of tumor and effector cells in fractional tumor-immune model for cancer treatment,” *Chaos, Solitons & Fractals*, vol. 141, Article ID 110321, 2020.
- [36] H. Singh, H. M. Srivastava, Z. Hammouch, and K. Sooppy Nisar, “Numerical simulation and stability analysis for the fractional-order dynamics of COVID-19,” *Results in Physics*, vol. 20, Article ID 103722, 2021.
- [37] M. Higazy, “Novel fractional order SIDARTHE mathematical model of the COVID-19 pandemic,” *Chaos, Solitons & Fractals*, vol. 138, 2020.
- [38] N. P. Dong, H. V. Long, and A. Khastan, “Optimal control of a fractional order model for granular SEIR epidemic with uncertainty,” *Communications in Nonlinear Science & Numerical Simulation*, vol. 88, Article ID 105312, 2020.
- [39] N. H. Tuan, H. Mohammadi, and S. Rezapour, “A mathematical model for COVID-19 transmission by using the Caputo fractional derivative,” *Chaos, Solitons & Fractals*, vol. 140, Article ID 110107, 2020.
- [40] Z. Zhang, “A novel covid-19 mathematical model with fractional derivatives: singular and nonsingular kernels,” *Chaos, Solitons & Fractals*, vol. 139, 2020.
- [41] R. P. Yadav, “A numerical simulation of fractional order mathematical modeling of COVID-19 disease in case of Wuhan China,” *Chaos, Solitons, and Fractals*, vol. 140, Article ID 110124, 2020.
- [42] N. Sweilam, S. Mekhlafi, S. Shatta, and D. Baleanu, “Numerical study for a novel variable-order multiple time delay awareness programs mathematical model,” *Applied Numerical Mathematics*, vol. 158, pp. 212–235, 2020.
- [43] A. K. Misra, A. Sharma, and J. B. Shukla, “Modeling and analysis of effects of awareness programs by media on the spread of infectious diseases,” *Mathematical and Computer Modelling*, vol. 53, pp. 1221–1228, 2011.
- [44] I. Podlubny, *Fractional Differential Equations*, Academic Press, New York, 1999.
- [45] C. Vargas-De-León, “Volterra-type Lyapunov functions for fractional-order epidemic systems,” *Communications in Nonlinear Science and Numerical Simulation*, vol. 24, no. 1, pp. 75–85, 2015.
- [46] J. Huo, H. Zhao, and L. Zhu, “The effect of vaccines on backward bifurcation in a fractional order HIV model,” *Nonlinear Analysis: Real World Applications*, vol. 26, pp. 289–305, 2015.
- [47] D. Matignon, “Stability results for fractional differential equations with applications to control processing,” in *Computational Engineering in Systems and Application Multi-Conference*, vol. 2, pp. 963–968, IEEE-SMC Proceedings, 1996.
- [48] A. E. Matouk, “Stability conditions, hyperchaos and control in a novel fractional order hyperchaotic system,” *Physics Letters A*, vol. 373, no. 25, pp. 2166–2173, 2009.
- [49] A. E. Matouk, “Complex dynamics in susceptible-infected models for COVID-19 with multi-drug resistance,” *Chaos, Solitons, and Fractals*, vol. 140, Article ID 110257, 2020.
- [50] A. Wolf, J. B. Swift, H. L. Swinney, and J. A. Vastano, “Determining Lyapunov exponents from a time series,” *Physica D: Nonlinear Phenomena*, vol. 16, no. 3, pp. 285–317, 1985.
- [51] K. Diethelm and N. J. Ford, “Analysis of fractional differential equations,” *Journal of Mathematical Analysis and Applications*, vol. 265, no. 2, pp. 229–248, 2002.
- [52] K. Diethelm and N. J. Ford, “A predictor-corrector approach for the numerical solution of fractional differential equations,” *Nonlinear Dynamics*, vol. 29, p. 3, 2002.
- [53] M.-F. Danca and N. Kuznetsov, “Matlab code for Lyapunov exponents of fractional-order systems,” *Int. J. Bifurcat. Chaos*, vol. 28, no. 5, Article ID 1850067, 2018.
- [54] H. Alahdal, F. Basingab, and R. Alotaibi, “An analytical study on the awareness, attitude and practice during the COVID-19 pandemic in Riyadh, Saudi Arabia,” *Journal of Infection and Public Health*, vol. 13, no. 10, pp. 1446–1452, 2020.
- [55] R. Tripathi, S. S. Alqahtani, A. A. Albarraq et al., “Awareness and preparedness of COVID-19 outbreak among healthcare workers and other residents of south-west Saudi Arabia: a cross-sectional survey,” *Frontiers in Public Health*, vol. 8, pp. 1–13, 2020.
- [56] Y. Alharbi, A. Alqahtani, O. Albalawi, and M. Bakouri, “Epidemiological modeling of COVID-19 in Saudi Arabia: spread projection, awareness, and impact of treatment,” *Applied Sciences*, vol. 10, no. 17, p. 5895, 2020.
- [57] <https://covid19awareness.sa/en/faqs-2>.